On the relationship between Fast Lyapunov Indicator and periodic orbits for symplectic mappings.

Elena Lega
Observatoire de Nice, Bv. de l'Observatoire, B.P. 4229, 06304 Nice cedex 4, France

Claude Froeschlé
Observatoire de Nice, Bv. de l'Observatoire, B.P. 4229, 06304 Nice cedex 4, France.

Abstract. The computation on a relatively short time of a quantity, related to the largest Lyapunov Characteristic Exponent, called Fast Lyapunov Indicator (Froeschlé, Lega and Gonczi 1997) allows to discriminate between ordered and weak chaotic motion and also, under certain conditions, between resonant and non resonant regular orbits (Froeschlé and Lega 2000). The aim of this paper is to study numerically the relationship between the Fast Lyapunov Indicator values and the order of periodic orbits. Using the two dimensional standard map as a model problem we have found that the Fast Lyapunov Indicator increases as the logarithm of the order of periodic orbits up to a given order. For higher order the Fast Lyapunov Indicator grows linearly with the order of the periodic orbits. We provide a simple model to explain the relationship that we have found between the values of the Fast Lyapunov Indicator, the order of the periodic orbits and also the minimum number of iterations needed to obtain the Fast Lyapunov Indicator values.

1. Introduction

In the last ten years many efforts have been made in order to have fast indicators for distinguishing between chaotic and regular motion, and also, in the case of regular motion, between resonant and non resonant orbits. Although the computation of the Lyapunov Characteristics Indicators (see Benettin et al. 1980 and Froeschlé 1984 for a detailed review) represents, from theoretical and from numerical point of view, the best suited method for distinguishing between ordered and chaotic motion, it doesn't allow to separate resonant from non resonant orbits.

This last task is very important for example when studying the global stability of a system. It is well known, from the celebrated Nekhoroshev's theorem (1977), that in a Hamiltonian system, satisfying some non–degeneracy condition, if the perturbation is small, orbits with initial conditions in a chaotic region do not diffuse in the action space. More precisely, given a perturbation parameter ϵ, only diffusion with a velocity exponentially small with respect to $-1/\epsilon$ can be expected.

When increasing the perturbation parameter the dynamic is no more controlled by the Nekhoroshev theorem. The system is described by the well known Chirikov (1960) overlapping criterium, which allows the resonant chaotic orbits to pass from one resonance to the other one, thus possibly giving large scale diffusion.

By a graphical representation of the distribution of tori, chaotic orbits and resonant regular orbits, i.e. of the Arnold web, it is possible to determine if the dynamics is controlled by Nekhoroshev theorem or by the Chirikov criterium.

Already Laskar (1993) and Lega and Froeschlé (1997) have managed, using respectively the frequency and the sup map analysis, to obtain a graphical representation of the Arnold web.

By computing, on a relatively short time, a quantity related to the largest Lyapunov Characteristic Exponent, Froeschlé and Lega (2000) have shown that this quantity, called Fast Lyapunov Indicator (hereafter FLI), distinguishes very well not only between chaotic and regular orbits but also between resonant regular orbits and non resonant ones.

Using the FLI, Froeschlé et al. (2000) have recovered easily and with a lot of details the Arnold web in a Hamiltonian system and also showed the transition from Nekhoroshev's regime to Chirikov's one. In the case of symplectic maps it is less clear if all the hypothesis of the Nekhoroshev theorem are satisfied. However, the numerical experiments (Froeschlé and Lega 2000, Guzzo et al. 2000), have shown structure and evolution very similar to those arising in Hamiltonian systems justifying the appellation of Nekhoroshev's like regime for the case of a map and the study of the transition from Nekhoroshev's like regime to Chirikov's one.

To summarize the present state of the art we can then say that the FLI is an indicator very sensitive to the dynamics of the orbits and because it is easy to be implemented and rapid in computation it turns out to be well adapted for studies concerning the global stability of a system.

Moreover, since the FLI have been shown to be very sensitive for the detection of resonant regular orbits we think that it is interesting to study numerically the relation existing between the FLI values and the order of periodic orbits. This is the aim of the present paper.

Taking the standard map as a model problem we show that there exists a relation $FLI(q) \simeq \log(q)$ between the FLI and the order q of the periodic orbits up to a given order q. Studying the Fibonacci sequence of the rational approximants to the golden torus we show that the FLI of periodic orbits becomes constant after a transient linear increase for an interval of time which grows with the order q.

We have also obtained that both the FLI values and the number of iterations which are necessary to obtain them are proportional to $\log(q)$ up to a given order. For higher order periodic Fibonacci orbits, both, the FLI values and the number of iterations to obtain them, increase linearly with the order.

The difference between the FLI values obtained for resonant regular orbits and the FLI values of circulation tori is explained through the properties of the differential rotation (Froeschlé and Lega 2000). In the case of periodic orbits there is no differential rotation and we have introduced a very simple model of linear elliptic rotation for explaining the relationship that we have found between the values of the FLI, the order of the periodic orbits and also the minimum number of iterations needed to obtain the FLI values.

In the light of the results of the simple model we have found that the FLI values obtained on the Fibonacci sequence are in very good agreement with the measure of the size of the Fibonacci islands (Lega and Froeschlé 1996, Locatelli et al. 2000), and hence with the description of the structure around an invariant KAM torus, the golden torus in this case, theoretically predicted by Morbidelli and Giorgilli (1995). We remark that the study of the neighbourhoud of the golden torus has been much easier with the FLI than with the frequency-map analysis as in Lega and Froeschlé (1996).

The paper is organized as follows. In Section 2 we recall the definition of the FLI for a mapping; in 3 we compute this indicator on some orbits of the two dimensional standard map. In Section 4 we obtain a relation between the FLI and the order of the periodic orbits. We compute the FLI on the sequence of Fibonacci periodic orbits in 5. In the same Section we introduce a simple model based on linear elliptic rotation which help us for discussing the results on the Fibonacci sequence. Conclusion and future developments are provided in 6.

2. The Fast Lyapunov Indicator revisited

When computing the Lyapunov Characteristics Indicators the attention is focused on the length of time necessary to get a reliable value of their limit, i.e. of the Lyapunov Characteristic Exponents, but very little importance has been given to the first part of the computation. In fact, this part was considered as a kind of transitory regime depending, among other factors, on the choice of an initial vector of the the tangent manifold.

Already in 1997 Froeschlé et al. have remarked that the intermediate values of a quantity related to the largest Lyapunov Characteristic

Indicator taken at equal times for chaotic, even slow chaotic, and ordered motion, allows to distinguish between them. This indicator, called Fast Lyapunov Indicator (FLI), turned out to distinguish also among ordered motions of different origins, like resonant and non resonant motion (Froeschlé and Lega 2000), despite the fact that in both cases the Lyapunov Characteristic Indicators converge to zero when t goes to infinity.

Given a mapping M from $\Re^n$ to $\Re^n$, an initial condition $\vec{x}(0) \in \Re^n$, and an initial vector $\vec{v}(0) \in \Re^n$ of norm 1, the FLI function $\bar{F}(\vec{x}(0), \vec{v}(0), t)$, t belonging to Z^+, is defined as:

$$\bar{F}(\vec{x}(0), \vec{v}(0), t) = \frac{1}{2N} \sum_{k=t-N}^{k=t+N-1} \log ||\vec{v}(k)|| \tag{1}$$

where the evolution of the vector $\vec{v}(t)$ is given by the set of coupled equations:

$$\begin{cases} \vec{x}(t+1) & = & M\vec{x}(t) \\ \vec{v}(t+1) & = & \frac{\partial M}{\partial \vec{x}}(\vec{x}(t))\vec{v}(t) \end{cases} \tag{2}$$

The running average on a set of N data was introduced in Froeschlé and Lega (2000) in order to smooth the oscillations of the norm of $\vec{v}(t)$ due to the distortion of the orbits.

For the same reason, in view to the study of very small resonant zones, like for instance the set of Fibonacci islands which approximate the golden torus, we slightly modify the definition of the FLI function F taking the maximum value that the norm of the tangent vector reaches up to time t:

$$F(\vec{x}(0), \vec{v}(0), t) = \sup_{0 \le k \le t} \log ||\vec{v}(k)|| \tag{3}$$

The advantage of the last definition when comparing different orbits is to be independent from the parameter N, i.e. from the portion of the of the orbit visited in the interval $[t-N, t+N-1]$ (Eq.1). Although the same N can be used when comparing resonances of small order, like in Froeschlé and Lega (2000), the parameter N should be adapted to the resonance order in view of fine studies like the analysis of the set of Fibonacci islands. The new definition (Eq.3) avoids us tedious calibrations of N as a function of the resonance order.

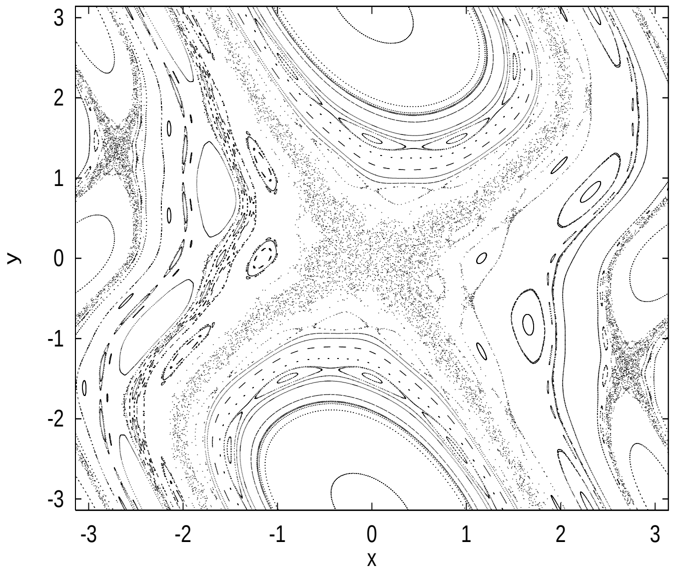

Figure 1. A set of orbits of the standard map for $\epsilon = 0.9$.

3. Application to the standard map

We consider as a model problem the two dimensional standard map (Froeschlé 1970, Lichtenberg & Lieberman 1983):

$$M = \left\{ \begin{array}{lcll} x(t+1) & = & x(t) + \epsilon \sin(x(t) + y(t)) & (\mathrm{mod} 2\pi) \\ y(t+1) & = & x(t) + y(t) & (\mathrm{mod} 2\pi) \end{array} \right. \tag{4}$$

Fig.1 displays orbits of the standard map of Eq.4 for $\epsilon = 0.9$.

For this value of the perturbing parameter the majority of tori have disappeared and the phase space shows a rich structure of chains of islands and chaotic orbits. Let us recall that the value of the perturbation parameter for which the last KAM torus is broken down is $\epsilon = 0.971635$ (Greene 1979, Olivero and Simó 1987, Laskar et al. 1992, Laskar 1995 and Mackay 1993),

For $\epsilon = 0.9$ we have computed the FLI (as in Eq.3) for four orbits of the standard map. For the chaotic orbit (Fig.2) with initial conditions $x(0) = 0.00001, y(0) = 0$, the FLI shows an exponential increase with time. In the case of a regular non resonant orbit with $x(0) = 2.13, y(0) = 0$ and of a regular resonant orbit with $x(0) = 1.2, y(0) = 1$ (the small chain of 4 islands plotted in Fig.1) the FLI grows linearly with time but with a different speed (Fig.2). In fact, because of the differential rotation, the norm of the vector $\vec{v}$ asymptotically grows as $||\vec{v}(t)|| \simeq \alpha t$, the coefficient α depending on the nature of the invariant

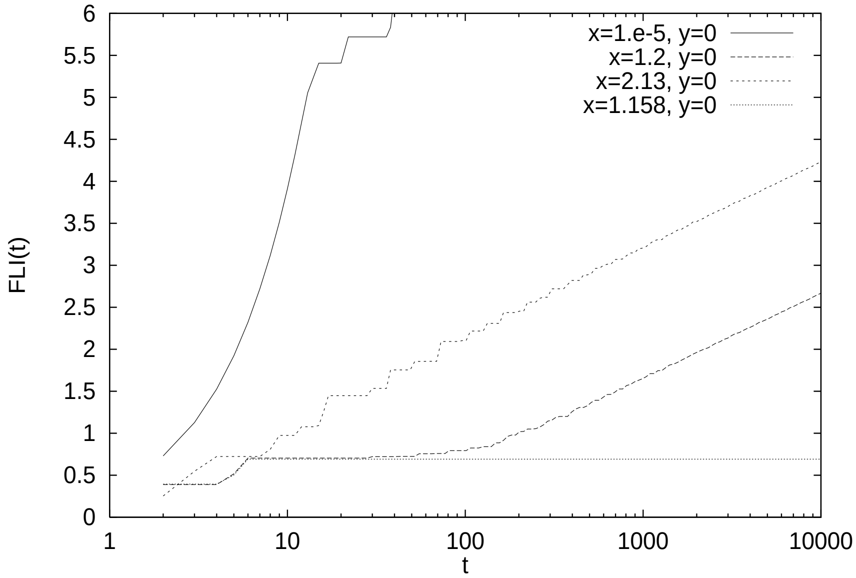

Figure 2. Variation of the Fast Lyapunov Indicator with time for four orbits of the standard map with $\epsilon = 0.9$. The upper curve is for a chaotic orbit with initial conditions $x(0) = 0.00001, y(0) = 0$, the second one is for a regular non resonant orbit with $x(0) = 2.13, y(0) = 0$ and the third one is for a regular resonant orbit with $x(0) = 1.2, y(0) = 1$. This orbit is plotted in Fig.1 and corresponds to a chain of 4 small islands. The curve with constant FLI is obtained for the corresponding periodic orbit of order $q = 4$ of initial conditions $x(0) = 1.158, y(0) = 0$.

curve (torus or libration island). In particular, inside a libration island the variation of the differential rotation is lower than inside a region of tori (for an heuristic analytic demonstration using an Hamiltonian system see Guzzo et al. 2000 and for numerical experiments see Froeschlé and Lega 2000). Therefore, since we plot the logarithm of the norm of $\vec{v}(t)$ against the logarithm of the time t we get parallel lines for the resonant and non resonant cases and these two regular dynamics are clearly distinguished.

The curve with constant FLI is obtained for the periodic orbit of order $q = 4$ of initial conditions $x(0) = 1.158, y(0) = 0$. The aim of this paper is to understand such peculiar behaviour of the FLI for periodic orbits.

We have started computing the FLI for a set of 10 000 initial conditions regularly spaced on the x-axis in the interval $[0, \pi]$. For each orbit $y(0) = 0$. Fig.3 shows what we call the FLI-map, i.e. the value of F after $t = 10\,000$ iterations against $x(0)$, $\vec{v}(0)$ being always taken in the direction of the x-axis. As shown by Foreschlé and Lega (2000) the values of F depend on the direction of $v(0)$ and the authors suggest to

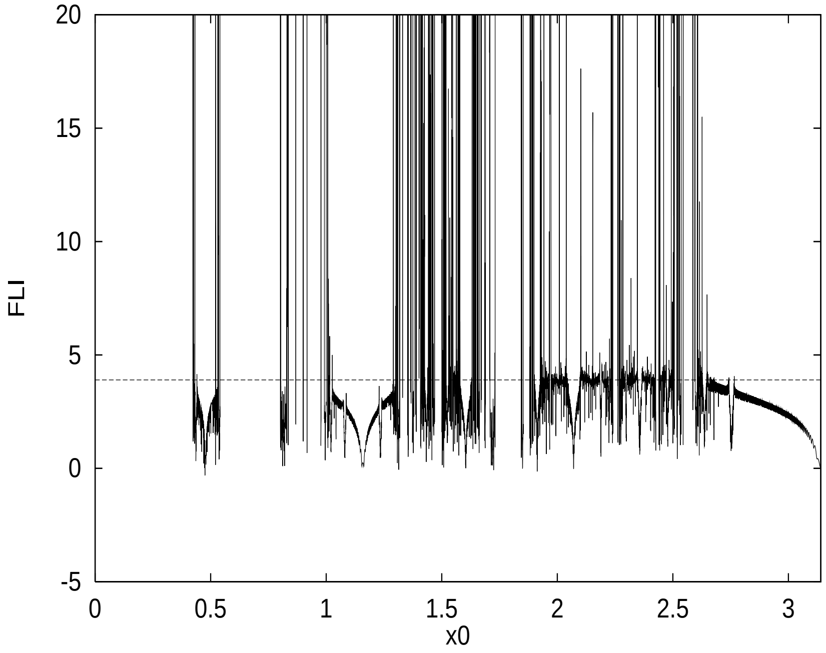

Figure 3. Variation of the FLI computed at $t = 10\,000$ iterations of the mapping, as a function of the initial action $x(0)$ for a set of 10 000 orbits regularly spaced in the interval $[0, \pi]$. The perturbation parameter is $\epsilon = 0.9$. The initial vector is $\vec{v}(0) = (1, 0)$ for the whole set of orbits. The threshold for the detection of islands $FLI = 3.9$ is also plotted.

take the same $v(0)$ for the whole set of orbits in order to compare their dynamical character.

In the same article it is explained, by considerations on the differential rotation, that the tori have all the same FLI value which is of the order of the logarithm of the number t of iterations since the norm of $v(0)$ grows linearly with t. Actually, a small number of orbits of Fig.3 appear to have $F \simeq 4$ in agreement with the fact that the majority of tori have disappeared for this value of the perturbation parameter.

Islands, as already observed in Fig.2, are identified by values of the FLI lower than the reference value of tori. In fact, the differential rotation inside a chain of islands turns out to be lower than between tori and its derivative becomes close to zero (Froeschlé and Lega 2000) towards the center of the islands. The minima of the FLI observed in Fig.3 are a quite good approximation for the center of the crossed islands.

Chaotic orbits have FLI greater than the reference value of tori. The computation has been stopped when $F > 20$. Such orbits have a large

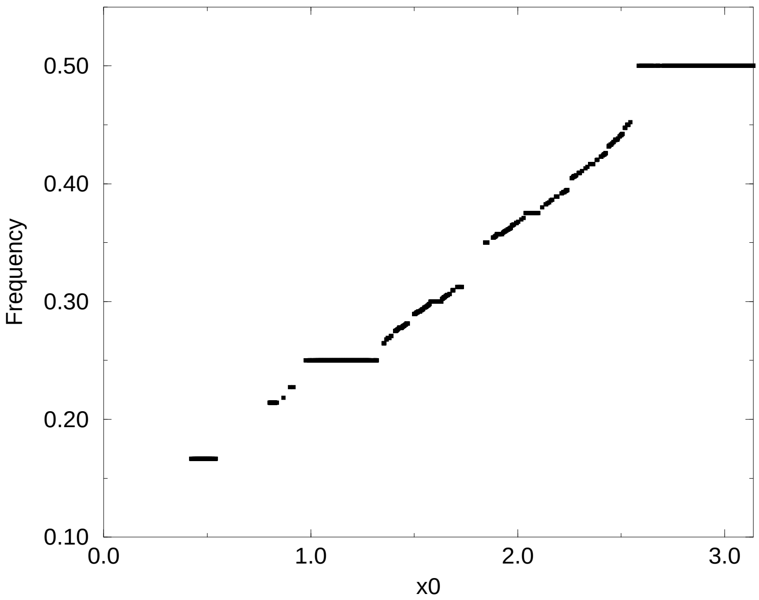

Figure 4. Frequency of orbits having FLI lower or equal than the threshold of 3.9 plotted as a function of the initial condition x_0.

positive Lyapunov Characteristic Indicator and for the purpose of this paper we do not need other informations about them.

4. Relationship between Fast Lyapunov Indicator and periodic orbits

As we said above we can associate regular resonant motion to all orbits of Fig.2 having FLI lower than the reference value of tori. Taking as a threshold the value $FLI = 3.9$, we obtain that 3772 of the previous analyzed set of 10 000 orbits are resonant regular orbits. For the corresponding set of initial conditions we have computed, using a fast method introduced in Lega and Froeschlé (1996), the frequency or rotation number.

Fig.4 shows the values of the frequency f computed using 10 000 iterations of the mapping for the set of 3772 orbits. As shown by Laskar et al. (1992) in the plot of the frequency as a function of the initial conditions, i.e. in the plot of the frequency-map, regular resonant orbits are identified by "plateaux" of constant frequency. Such "plateaux" appear clearly in Fig.4, for example the large one for orbits with initial conditions in the interval $0.95 < x(0) < 1.3$, $y(0) = 0$, corresponds to the chain of four islands of Fig.1 surrounding the periodic orbit

$p/q = 1/4$ of initial conditions $x(0) = 1.158$, $y(0) = 0$. The sensitivity of the FLI allows also to find very small chains of islands, the small "plateaux" of Fig.4. Actually, at this resolution it is quite difficult, at least visually, to distinguish on the frequency-map small "plateaux" from a monotonic increase of the frequency associated to invariant tori. We have developed in continued fraction the set of 3772 frequencies obtaining for each of them a rational representation p/q, $p, q \in Z^+$ thus confirming the detection of regular resonant motion by the FLI method.

Fig.5 shows the relation between the FLI values and the order q of the resonance obtained by the development in continued fraction of the orbits's frequencies. The vertical lines correspond to the set of values of the FLI of a given chain of islands. For example the line at $q = 2$ is for the set of initial conditions of the chain of 2 islands of Fig.1 whose center is the periodic orbit of coordinates $[\pi, -\pi]$, $[\pi, 0]$. The minimum value of the FLI for each chain of islands corresponds to an orbit close to the periodic orbit. For the case considered, $p/q = 1/2$, the FLI is 0.39 for an orbit with initial conditions: $x(0) = 3.1396$ $y(0) = 0$ very close to the periodic orbit: $x(0) = \pi$ $y(0) = 0$.

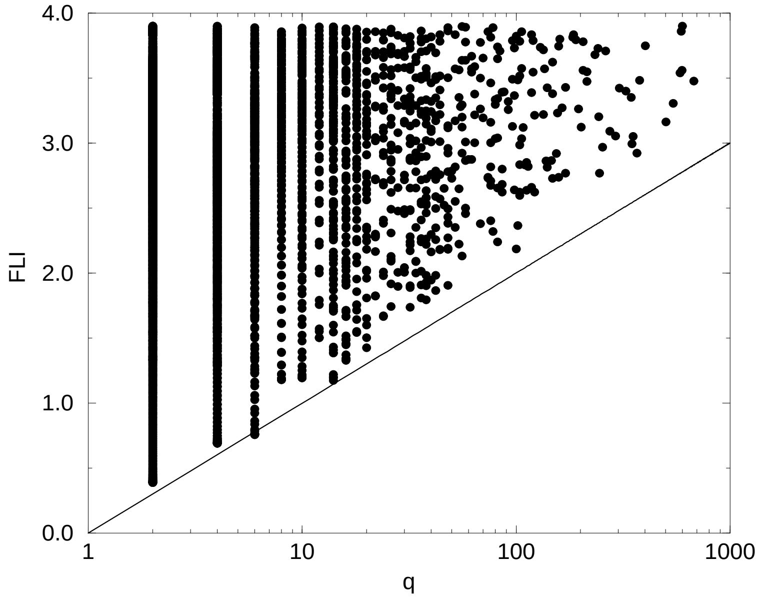

Figure 5. Values of the FLI corresponding to resonant orbits, i.e. to orbits of Fig.2 having FLI lower or equal to 3.9, plotted against the order of the resonance. This latter has been obtained by a development in continued fraction of the rotation number of the orbit. The straight line is $FLI = \log(q)$.

Considering the minima of the FLI against the order q of the periodic orbits we obtain numerically that the such values behaves like $\log(q)$ (the straight line on Fig.5).

5. A fine study of the Fibonacci sequence

In order to investigate more precisely the relationship obtained above between the FLI and the order of periodic orbits, we have computed the FLI as a function of time for a particular set of periodic orbits, the Fibonacci sequence.

Let us recall that the Fibonacci sequence is the set of the successive terms p_k/q_k obtained when developing the golden number through the continued fraction process and therefore is the sequence which best approximates[1] the golden number .

As explained in Lega and Froeschlé (1996), because of the smallness of the denominators the amplitude of the perturbation associated to the Fibonacci terms is large. This make the sequence a good candidate in view to the study of regular resonant motion, and in particular of the corresponding periodic orbits, up to a large order q. Such terms are also further from the golden number than any other set p_k/q_k from its corresponding irrational number. This is the origin of the strength of the golden torus, i.e. of the last KAM torus of the standard map of Eq.4 which, as we said in Section 3, is broken down for $\epsilon = 0.971635$.

Fig.6 shows the variation of the frequency as a function of the distance to the golden torus for $\epsilon = 0.9715$, i.e. very close to the perturbation parameter of the breakdown of the golden torus. More precisely we plot the logarithm of the absolute value of the difference between the frequency f of an orbit and the frequency fg of the golden torus.

The frequency is computed, using a fast method introduced in Lega and Froeschlé (1996), for a set of 20 000 orbits with $y(0) = 0$ and $x(0)$ regularly spaced on a logarithmic scale from $|x(0) - xg| = 10^{-9}$ to $|x(0) - xg| = 1$, xg being the action of the golden torus (when the angle yg is 0). The number of iterations used is suited to the precision required for the computation of the frequency and goes from $5\,10^6$ iterations for the orbits with $10^{-9} < |x(0) - xg| < 10^{-8}$ to 10^4 iterations for the orbits with $10^{-4} < |x(0) - xg| < 1$.

The set of Fibonacci terms that we analyze in the present paper is labeled in the Figure by the corresponding values of q_k. Far from the golden torus we can see only libration islands (the “plateaux” in

[1] We say that p/q is a best approximation of x if $|qx - p| < |q'x - p'|$ for all p', q' such that $0 < q' \leq q$ and $p'/q' \neq p/q$.

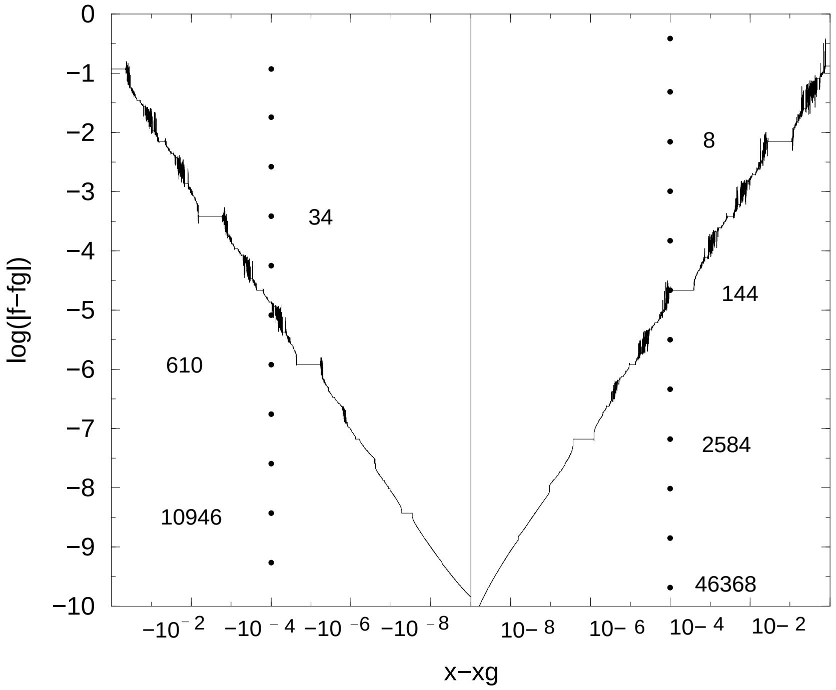

Figure 6. Logarithm of the absolute value of the difference between the frequency f of an orbit and the frequency fg of the golden torus as a function of the distance to the golden torus for the standard map with $\epsilon = 0.9715$. The filled circles in the figure correspond to the values $\log|f - fg|$ of the Fibonacci sequence. The set of Fibonacci terms that we analyze in the present paper is labeled in the Figure by the corresponding values of q_k.

the Figure) and chaotic zones (the noisy variations of the frequency). Starting from the resonance term 1597/2584 a surprisingly clear change of regime occurs: only tori remain (the monotonic variation of the frequency) sometimes interrupted by small libration islands and small vertical jumps (the crossing of thin separatrices). This change of regime perfectly agrees with the representation given by a theorem of Morbidelli and Giorgilli (1995) about the dynamics in a small neighborhoud of a noble torus.

The same features appear in Fig.7 where the FLI is plotted as a function of the distance to the golden torus for $\epsilon = 0.9715$, and for the same number of iterations used for the frequency analysis of Fig.6. The structures detected seem to be even more rich (because this indicator is very sensitive even to very small chaotic zones) and the change of regime appears very clearly in agreement with the results on the frequency map.

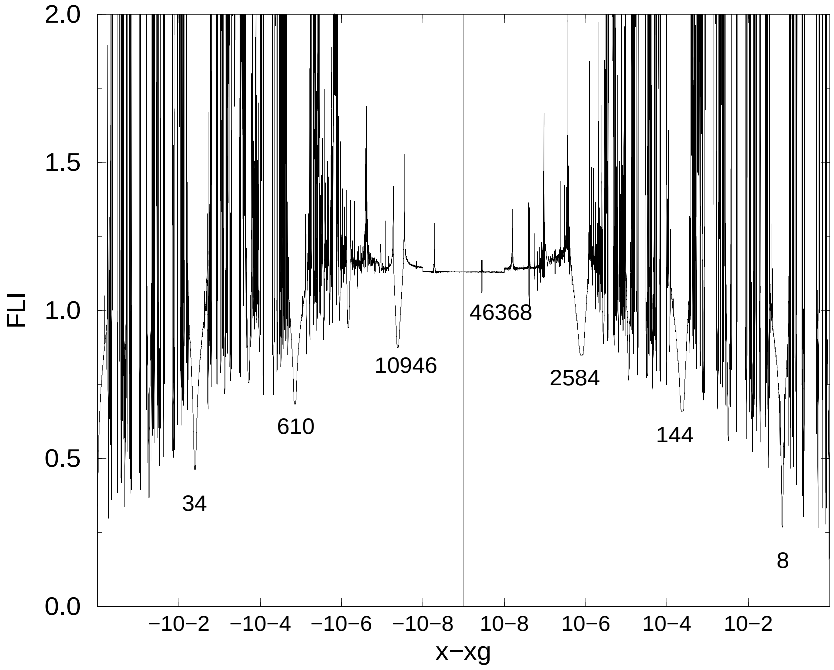

Figure 7. Variation of the FLI as a function of the distance to the golden torus for the standard map with $\epsilon = 0.9715$. The set of Fibonacci terms that we analyze in the present paper is labeled in the Figure by the corresponding values of q_k.

Fig.8 shows the variation with time of the FLI for a set of periodic orbits belonging to the Fibonacci sequence for the standard map with $\epsilon = 0.9715$. As obtained in Fig.2 the FLI of periodic orbits, after a transitory linear increase (which is very short for the periodic orbit of order 4 of Fig.2) becomes constant, i.e. the norm of $\vec{v}(t)$ reaches some maximum value.

Let us consider the trivial case of the two dimensional standard map with $\epsilon = 0$. In this case the norm of the vector $\vec{v}$ is equal to

$$||(\vec{v}(t)|| = \sqrt{t^2 v_x(0)^2 + v_y(0)^2} \tag{5}$$

independently on the initial conditions, i.e. for a given initial vector of components $\vec{v}(0) = (v_x(0), v_y(0))$ the FLI is the same for both a periodic and a quasi-periodic orbit. The difference with the perturbed case is that in this last case a periodic orbit is surrounded by quasi-elliptic regular resonant orbits. We think that the reason why the FLI becomes constant for the periodic orbits in the perturbed case must be found exactly on the fact that the linearized orbits in the phase space around the periodic orbits are elliptic. Therefore, in order to study the

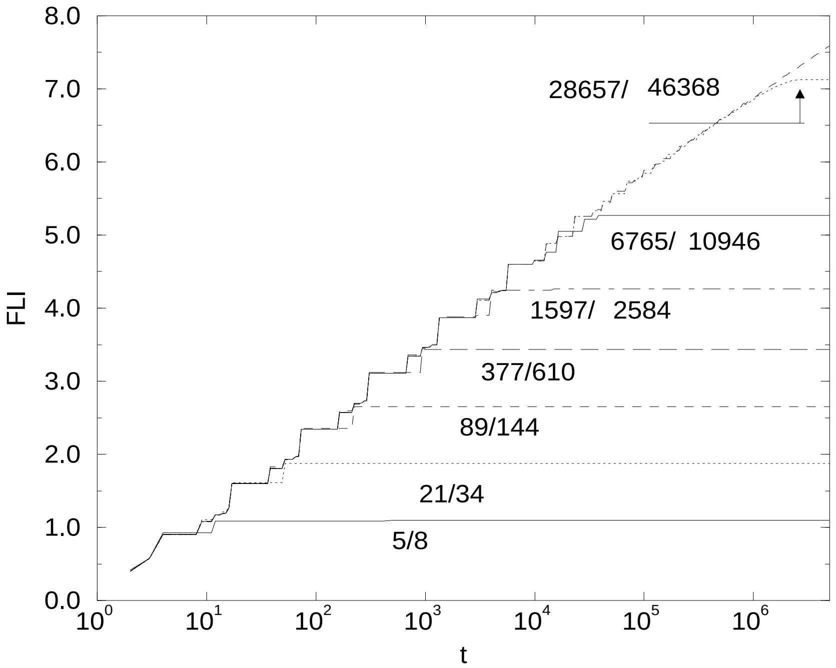

Figure 8. Variation with time of the FLI for a set of periodic orbits belonging to the Fibonacci sequence for the standard map with $\epsilon = 0.9715$. The rational ratios p/q of each term are written in the Figure near the corresponding FLI curve. The FLI curve which grows linearly with time all over the interval $0 < t < 5\,10^6$ iterations is obtained for the golden torus.

behavior of the FLI for periodic orbits we will introduce below a simple are-preserving mapping of linear elliptic rotation.

In Fig.8 the FLI curve which grows linearly with time all over the interval $0 < t < 5\,10^6$ iterations is obtained for the golden torus.

It is interesting to observe that, during the transitory linear increase, the FLI values obtained for the whole set of Fibonacci terms coincide with those of the golden torus. In fact, the ellipses surrounding the periodic orbits are more and more elongated for increasing order q, they become almost tangent to the near invariant tori, while the chaotic zone surrounding the islands shrinks to zero. Therefore, at least for high order resonances ($q \geq 610$) the FLI for a transient period of time is the same for the periodic orbits and for the near tori because of the continuity of the tangent manifold of Eq.2 (we recall that the FLI is the same for all tori, so the curve of Fig.8 obtained for the golden torus is valid for all invariant tori). Surprisingly, this argument based on continuity seems to hold also for lower order periodic orbits, although the chaotic zone surrounding the libration islands is large (Fig.6 and Fig.7) and probably a very small number of tori remains.

We can observe in Fig.8 that both the duration of the transitory linear increase of the FLI and its maximum and constant value seem to be related to the order q of the periodic orbits.

In what follows we introduce a simple model in order explain the observed features: the linear increase of the FLI, the constancy after a transient interval of time and the dependence on the order q.

5.1. A simple model

A small libration island close to the periodic orbit can be interpreted, through linearization, by an ellipse of ratio $\gamma = a/b$ between the semi-major axis a and the semi-minor axis b. Since there is no differential rotation in the case of periodic orbits, we consider a model without differential rotation. Let us define the following area-preserving mapping:

$$N = \left\{ \begin{array}{lcl} x(t+1) & = & x(t)\cos(\alpha) - \gamma y(t)\sin(\alpha) \\ y(t+1) & = & \frac{1}{\gamma}x(t)\sin(\alpha) + y(t)\cos(\alpha) \end{array} \right. \tag{6}$$

where α is the mean rotation angle of the radius vector of the ellipse.

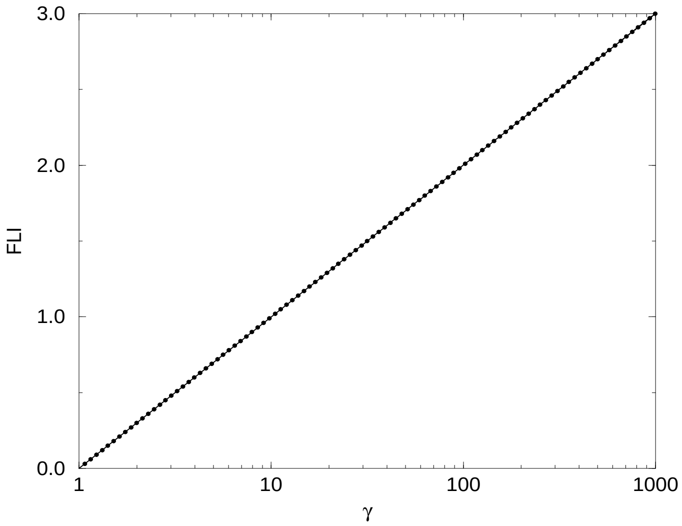

Figure 9. Variation of the FLI with γ for the area-preserving mapping model of Eq.6. Results are in perfect agreement with the expected behavior $FLI = \log(\gamma)$.

In fact, since this mapping is area preserving, for a given number of iterations the density of the points will be higher for the regions further from the center and the angle α turns out to be a mean rotation angle as it is for the islands of the standard mapping.

A vector of the tangent manifold corresponding to an elliptic orbit of Eq.6 is contracted and dilated along the ellipse, but its norm, because there is no differential rotation, cannot grow more than a maximum value which should be exactly γ. Fig.9 shows the variation of the FLI with the parameter γ for $t = 10000$ and γ belonging to the interval $1 < \gamma < 1000$. Results are in perfect agreement with the expected behavior $FLI = \log(\gamma)$.

Let us remark that results of Fig.9 are invariant for increasing values of the time t, i.e. the FLI values plotted correspond to the stable values of Fig.8.

A question remains about the transitory regime in which the FLI grows linearly with time.

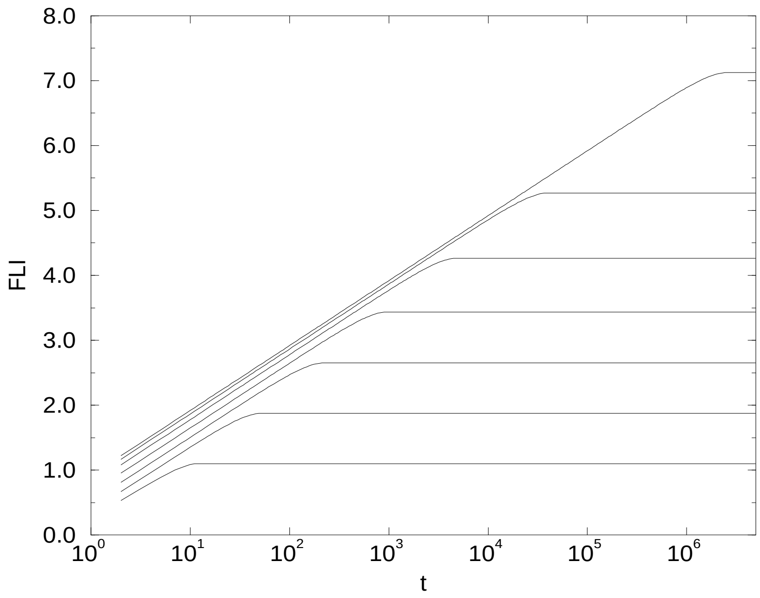

Figure 10. Variation of the FLI with time for the area-preserving mapping model of Eq.6. The values of γ correspond to the final FLI values of the Fibonacci periodic orbits of Fig.8. The rotation angles are the inverse of the time necessary for the FLI to reach its maximum value for the Fibonacci terms analyzed in Fig.8. Results of Fig.8 are well reproduced by the model.

Actually, in order to reach its maximum value, the vector $\vec{v}(t)$ has to "visit" the ellipse from the the semi-minor to the semi-major axis, i.e. has to rotate of at least an angle of 90 degrees. In Fig.10 we have plotted the evolution of the FLI with time for 7 orbits of the mapping of Eq.6 having γ values such that $\log(\gamma) \equiv FLI$ of the 7 Fibonacci periodic orbits analyzed in Fig.8. For the rotation angles we have considered $\alpha = 90/tFLI$ degrees, where $tFLI$ is the time necessary for the FLI to become constant for the 7 orbits of Fig.8. Results of Fig.10 reproduce very well the evolution of the FLI with time of the 7 Fibonacci periodic orbits, confirming the validity of the simple model for explaining the behavior of the FLI for periodic orbits.

5.2. The results of the simple model as a guideline for the study of the FLI on the Fibonacci set

In the light of the results obtained with the simple model, we can test if the maxima of the FLI for periodic orbits correspond to the geometric parameter $\gamma = a/b$ and if the time of transition to reach the maximum FLI value agrees with the kinematic parameter α corresponding to the mean rotation angle.

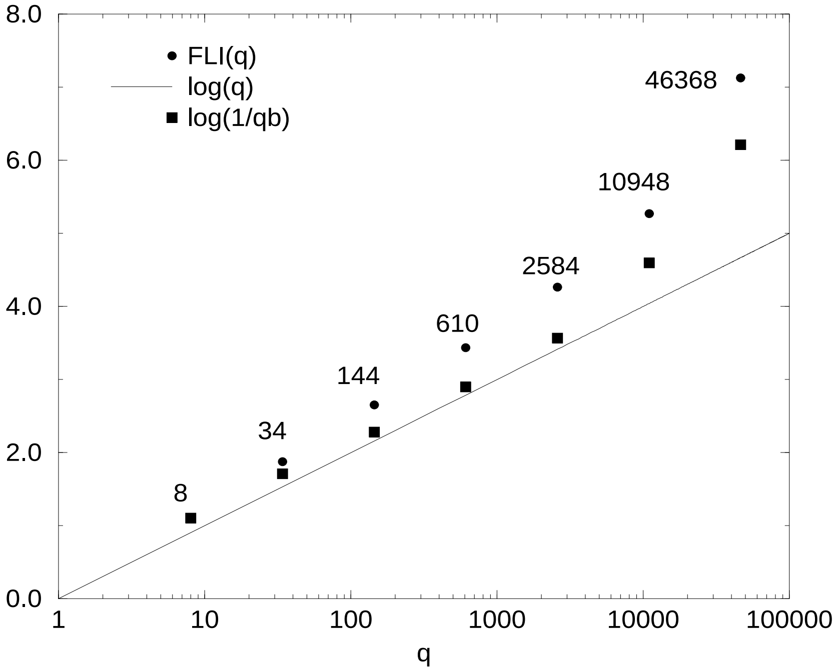

Figure 11. FLI values plotted against the order q for the set of Fibonacci periodic orbits of the standard map with $\epsilon = 0.9715$ analyzed in Fig.8. The straight line is the line $FLI = \log q$. The points labeled by a square correspond to the $\log(a/b)$, i.e. the expected values for the FLI, with $a = 1/q$ and b measured with the frequency-map analysis of the Fibonacci sequence (from Lega and Froeschlé 1996).

Fig.11 shows the relation between the FLI and the order q of the periodic orbits. The behavior of the FLI as $log(q)$ is quite well respected up to the order $q = 610$, i.e. by the first four periodic orbits. Then a sort of change of regime occurs.

The semi-major axis a decreases with the order like $1/q$. Concerning the semi-minor axis b, it has been obtained by numerical experiments (Lega and Froeschlé 1996) on the two dimensional standard map that its size decreases like the distance from the golden torus up to $q = 610$. Since the distance of a Fibonacci island from the golden torus behaves like $1/q^2$ we expect $a/b \simeq q$, i.e. $FLI \simeq \log(q)$, in agreement with the results of Fig.11.

Then, for higher order resonances, $q \geq 2584$, in a very small neighborhoud of the golden torus, the size b of the Fibonacci islands has been shown (Lega and Froeschlé 1996, Locatelli et al. 2000) to decrease exponentially as theoretically predicted in a theorem by Morbidelli and Giorgilli (1995). Taking the values of b measured by Froeschlé and Lega (1996) using the frequency map analysis we have plotted in Fig.11 the values $\log\gamma(q) \equiv \log(a(q)/b) \equiv \log(1/qb)$. It turns out that the relation $FLI(q) = \log\gamma(q)$ expected from the simple model of Eq.6 is quite well respected from the results of Fig.11. Although the behavior is the expected one, we can observe that the difference between the FLI values and the numerical values $\log(a(q)/b)$ with b taken from Lega and Froeschlé (1996) increases in the exponential regime ($q \geq 2584$). This fact suggest us to make finer studies, out of the purpose of this paper, of the exponential decrease of the volume of high order resonances.

However, the change of regime on b from a power low to an exponentially small b occurs also for the FLI, but the results are very much simpler to obtain than the measure of "plateaux" by the frequency analysis. Although a finer study is out of the purpose of this paper we think that the FLI method is well suited for a better comprehension of the dynamical properties of the standard map.

Fig.12 shows the time necessary for the FLI to become constant against the order q of the periodic Fibonacci orbits. A linear relation between the FLI and the order q holds up to the order $q = 610$ of the Fibonacci term $p/q = 377/610$. Then, again a sort of change of regime occurs.

Following the results of Fig.10, we have measured the kinematic parameter, i.e. the mean rotation angle using a method introduced by Contopoulos and Voglis (1997) and called twist angle. In fact, the twist angle has been shown (Froeschlé and Lega 1998) to give directly, in the case of regular resonant orbits, the frequency, or rotation angle measured by an observer in the center of the island. Let us call theoretical time, the time necessary for a vector to turn of an angle of 90 degrees, i.e. the ratio $tt = 90/\alpha$, α being the mean rotation angle. Fig.13 shows a surprisingly good agreement between the theoretical time and the

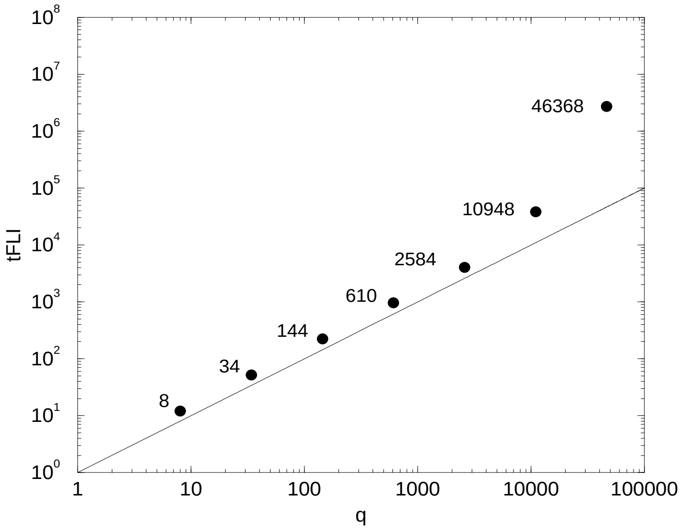

Figure 12. Time necessary for the FLI (tFLI) to become constant against the order q of the periodic orbits for the set of Fibonacci periodic orbits of the standard map with $\epsilon = 0.9715$ analyzed in Fig.8. The straight line is $tFLI = q$.

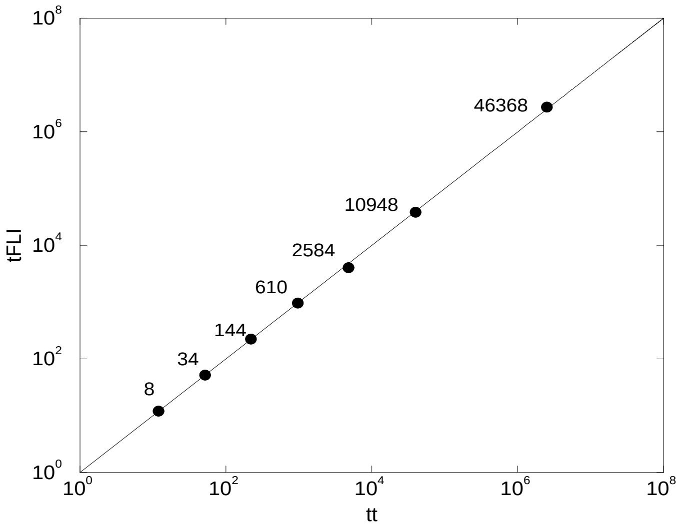

Figure 13. Time necessary for the FLI to become constant (tFLI) against the time expected (tt) for the vector $\vec{v}(t)$ to reach its maximum allowed value for the periodic Fibonacci orbits analyzed in Fig.8. The straight line is $tFLI = tt$

experimental time of Fig.8 necessary for the FLI to reach its maximum value. The rotation angle turns out to be a quantity invariant to the change of regime observed for the size of the islands.

The model of linear elliptic rotation seems therefore to fit very well for the comprehension of the behavior of the FLI on periodic orbits.

6. Conclusion

The Fast Lyapunov Indicator (Froeschlé, Lega and Gonczi 1997) was shown to be particularly sensitive for the distinction between regular and chaotic, even slow chaotic orbits. Recently, it has been shown (Froeschlé and Lega 2000) that this indicator is also powerful for distinguish between resonant regular orbits and invariant tori. In the same article an explication for this behavior is given based on an argument related to the differential rotation.

Thanks to this property (Froeschlé et al. 2000) have obtained a detailed representation of the Arnold web on a suitable Hamiltonian system with 3 degrees of freedom and on a 4 dimensional symplectic mapping (Froeschlé and Lega 2000). The crucial question of the global stability of the system is also discussed, and an interval of transition between the exponentially long stable Nekhoroshev regime and the diffusive Cihirkov regime is also provided.

In Froeschlé et al. (2000) it was shown that the FLI had minimum values near the center of libration islands, i.e. seemed to be well suited also for the detection of periodic orbits. In this paper we have studied the FLI for periodic orbits showing that the FLI behaves like $\log q$, q being the order of periodic orbits. The application on a particular set of periodic orbits, the Fibonacci sequence which approximate the golden torus, has confirmed this result up to a given order q; for higher orders the size of the islands starts to shrinks exponentially to zero. The order q observed for the change of regime on the FLI is in perfect agreement with the one previously obtained (Lega and Froeschlé 1996, Locatelli et al. 2000) on the size of the Fibonacci islands.

We have observed that the FLI for periodic orbits reaches a maximum value after a given time t, and we have shown that this time corresponds very well to the time necessary for a vector to “visit” the elliptic orbits of the phase space from its semi-minor to its semi-major axis.

We have interpreted our results introducing a simple area-preserving model of linear elliptic rotation obtaining a good agreement between the FLI and both the geometric and the kinematic parameters introduced to explain both the maximum FLI value and the time necessary to reach it.

We have obtained encouraging results up to now on the standard mapping. Since this mapping can be considered as a paradigm model for the study of dynamical systems, in particular because of the richness of its structures, we intend to use the method for studies of physical interest like for example the three body-problem or the dynamic of stars inside a galaxy or even for problems of stability in celestial mechanics. Moreover, we also intend to use the method, thanks to its sensitivity, for a better comprehension of the properties of the standard map itself. In fact, the analysis of the Fibonacci sequence made in the present paper, allowed us to find in a much simple way, results in agreement with previous fine studies of the mapping (Lega and Froeschlé 1996 and references therein, Locatelli et al. 2000) and we think worth full to try to get an even finer exploration of the neighborhoud of an invariant torus.

Acknowledgments

We are indebted to prof. Antonio Giorgilli for many discussions and suggestions.

References

1. G. Benettin, L. Galgani, A. Giorgilli, and J.M. Strelcyn. Lyapunov characteristic exponents for smooth dynamical systems; a method for computing all of them. *Meccanica*, **15**:Part I : theory, 9–20 – Part 2 : Numerical applications, –21–30, (1980).
2. B. V. Chirikov. *Plasma Phys.*, **1**:253, (1960).
3. G. Contopoulos and N. Voglis. A fast method for distinguishing between order and chaotic orbits. *Astron. Astrophys.*, **317**:73–82, (1997).
4. C. Froeschlé. A numerical study of the stochasticity of dynamical systems with two degrees of freedom. *Astron. Astrophys.*, **9**:15–23, (1970).
5. C. Froeschlé. The Lyapunov characteristic exponents and applications. *Jornal de Méc. théor. et apll.*, Numero spécial:101–132, (1984).
6. C. Froeschlé and E. Lega. Twist angles: a fast method for distinguishing islands, tori and weak chaotic orbits. Comparison with other methods of analysis. *AA*, **334**:355–362, (1998).
7. C. Froeschlé, E. Lega, and R. Gonczi. Fast Lyapunov indicators. Application to asteroidal motion. *Celest. Mech. and Dynam. Astron.*, **67**:41–62, (1997).
8. C. Froeschlé C. and E. Lega. On the structure of symplectic mappings. The Fast Lyapunov indicator: a very sensitive tool. *Celest. Mech. and Dynamical Astronomy*, in press, (2000).
9. C. Froeschlé, M. Guzzo and E. Lega. Graphical evolution of the Arnold's web: from order to chaos. *Science*, **289-N.5487**:2108–2110, (2000).

10. J.M Greene. A method for determining a stochastic transition. *J. Math. Phys.*, **20**:1183, (1979).
11. M. Guzzo, E. Lega and C. Froeschlé. Stable and unstable chaos. Recent numerical tools for the transition from Nekhoroshev to Chirikov regimes. in preparation, 2000.
12. J. Laskar. Frequency analysis for multi-dimensional systems. Global dynamics and diffusion. *Physica D*, **67**:257–281, (1993).
13. J. Laskar. Frequency map analysis of an Hamiltonian system. *Workshop on Non-Linear Dynamics in Particle Accelerators*, Arcidosso, September 1994.
14. J. Laskar, C. Froeschlé, and A. Celletti. The measure of chaos by the numerical analysis of the fundamental frequencies. Application to the standard mapping. *Physica D*, **56**:253, (1992).
15. E. Lega and C. Froeschlé. *Fast Lyapunov Indicators. Comparison with other chaos indicators. Application to two and four dimensional maps.* in The Dynamical Behaviour of our Planetary System., Kluwer academ. publ., J.Henrard and R.Dvorak eds., (1997).
16. E. Lega and C. Froeschlé. Numerical investigations of the structure around an invariant KAM torus using the frequency map analysis. *Physica D*, **95**:97–106, (1996).
17. W.J. LeVeque. *Fundamentals of Number Theory.* Addison-Wesley Publishing Company, (1977).
18. A.J. Lichtenberg and M.A. Lieberman. *Regular and Stochastic motion.* Springer, Berlin, Heidelberg, New York, (1983).
19. U. Locatelli, C. Froeschlé, E. Lega, and A. Morbidelli. On the relationship between the Bruno function and the breakdown of invariant tori. *Physica D*, **139**:48–71, (2000).
20. R.S. MacKay. *Renormalisation in Area Preserving Maps.* World Scientific, (1993).
21. K. Mahler. *Lectures on Diophantine Approximations.* (1957).
22. A. Morbidelli and A. Giorgilli. Superexponential stability of KAM tori. *J. Stat. Phys.*, **78**:1607, (1995).
23. N.N. Nekhoroshev. Exponential estimates of the stability time of near-integrable Hamiltonian systems. *Russ. Math. Surveys*, **32**:1–65, (1977).
24. A. Olivera and C. Simó. An obstruction method for the destruction of invariant curves. *Physica D*, **26**:181, (1987).